JOURNAL OF APPLIED ELECTROCHEMISTRY 1 (1971) 53–63

Electrochemical behaviour and glass formation in molten bisulphates

M. D. INGRAM, J. A. DUFFY, S. M. FORBES

Department of Chemistry, University of Aberdeen, U.K.

Received 25 September 1970

Molten bisulphates form an interesting class of low-temperature fused salts which quench to form glasses; some technical and theoretical applications of these systems are discussed. The $NaHSO_4$–$KHSO_4$ eutectic (46·5% $KHSO_4$, m.p. 125°C, T_g 25°C) is easy to study since at lower temperatures decomposition of the melt is retarded and supercooling readily occurs. The solvent properties of this eutectic towards both inorganic and organic solutes have been investigated. The oxidation states available to transition and post-transition metals were studied spectrophotometrically and voltametrically; the results show a very restricted pattern of redox chemistry. The (abbreviated) electrochemical series is $V(V)/V(IV) > Mn(III)/Mn(II) > H(I)/H_2(O) > Ag(I)/Ag(O) > Mo(VI)/Mo(V) > Hg(I)/Hg(O) > Cu(II)/Cu(O) > Zn(II)/Zn(O)$. The Hammett acidity function, H_0, was measured as in the range -1 to -2. Various factors influencing redox reactions in the melt are discussed.

Introduction

Molten bisulphates form an interesting group of low-temperature melts which deserve further study. Thus Rogers and Ubbelohde [1] investigated the physical properties of bisulphate melts and have identified some convenient eutectic compositions in the $NaHSO_4$–$KHSO_4$ system (m.p. 125°C, 46·5% $KHSO_4$) and in the NH_4HSO_4–$KHSO_4$ system (m.p. 110·5°C, 17% $KHSO_4$).

Until recently, published papers on molten bisulphates have been largely concerned with electrode processes. Thus, Tajima *et al.* [2] electrolysed potassium bisulphate and various mixed melts using platinum electrodes, and found that the volumes of gases evolved at the cathode and anode were in the ratio 2 : 1. By analogy with aqueous systems it was concluded that the gases evolved are cathodic hydrogen and anodic oxygen; sulphur trioxide, which is also produced at the anode, dissolves in the melt. The overpotential phenomena associated with hydrogen evolution, and oxygen evolution and reduction at various metal electrodes, have been examined in a series of papers by Shams El Din [3] and Arvia and his co-workers [4–9]. Arvia and Videla also described a reversible H_2 electrode for use in molten bisulphates and evaluated a table of rest potentials for various metals. The results of Arvia [4–9] point to a strong resemblance between the electrode phenomena in aqueous solutions and bisulphate melts, and it is interesting to speculate on the possible use of these melts as electrolytes in medium-temperature fuel cells.

One of the main problems in working with bisulphate systems is their thermal instability. Loss of water and sulphur trioxide lead to the formation of pyrosulphate and ultimately sulphate, thus

$$2\,MHSO_4 \rightarrow M_2S_2O_7 + H_2O;$$
$$M_2S_2O_7 \rightarrow M_2SO_4 + SO_3.$$

Several groups of workers have studied these decomposition reactions [1, 10, 11, 12]. Walrafen and co-workers [12] used Raman spectroscopy to examine the species present in potassium bisulphate melt as a function of temperature. It was observed that above 300°C conversion of

HSO_4^- to $S_2O_7^{2-}$ becomes significant but that no SO_4^{2-} appears in the melt below 500°C. However, at temperatures of *c.* 200°C, this decomposition reaction is probably very slow. It must be pointed out that much of the previous work on electrode overpotentials involved temperatures above 300°C, and it seems possible that those results were affected by melt decomposition.

Molten bisulphates also readily supercool and form glasses [13, 14]. Notably, melts close to the eutectic composition in the $NaHSO_4$–$KHSO_4$ system show almost no tendency to crystallize on cooling. These glass-melt systems are interesting both from the theoretical and practical standpoints. Thus, Angell *et al.* [15] have shown how transport measurements (conductance, viscosity, etc.) in the 'low-temperature region' of a fused salt ($T<2T_g$ where T_g is the glass-transition temperature (°K)) can provide useful data for testing theories of glass formation. Moreover, Bose *et al.* [16] have shown recently that close to the glass transition temperature interesting phenomena are encountered. In the $NaHSO_4$–$KHSO_4$ melts it should be possible to explore this region of behaviour in a convenient temperature range (see below) and without interference from crystallization.

Bisulphate glasses at present do not find technical application but there are some interesting possibilities. The current concern with 'conservation' has led to a search for biodegradable polymers for use in disposable containers. It is conceivable that bisulphates could be used as water-soluble components in disposable glasses. Bisulphate glasses are in fact only slowly soluble in hot water and might be useful for 'on-line' control of pH in industrial processes. The melts also have good adhesive properties, and it is possible to stick silica plates together to yield a composite glass which is transparent well into the ultraviolet region (up to 50,000 cm^{-1}).

Molten salts in general form a class of nonaqueous solvents, but until now there has been little attempt to consider bisulphate melts from this standpoint. The only previous work has been (*i*) an examination of the sites available to transition metal ions by d–d [14, 17] and charge transfer [18] spectra and (*ii*) a study of ligand substitution reactions in complexes of chromium(III) and cobalt(III) dissolved in the melt [19]. This neglect of the 'solvent' properties of molten bisulphates is surprising in view of their importance in the extraction of platinum-group metals and possible participation in reactions on the vanadium catalyst used in sulphuric acid manufacture.

In this paper we discuss the redox and related properties of the $NaHSO_4$–$KHSO_4$ solvent. Oxidation–reduction reactions are observed by voltametry and electronic absorption spectroscopy, and the results are discussed in terms of the electrochemical series and the Hammett acidity function of the medium. The range of bisulphate melts which form glasses and the appropriate glass-transition temperatures are also reviewed. It is intended to use this information in the future as a basis for more sophisticated studies of bisulphate melts and glasses.

Experimental procedure

Materials

AnalaR sodium and potassium bisulphates were used, as supplied by B.D.H., without further purification. These reagents were oven dried at 140° for 1 h, ground together and melted immediately before use. Most electrochemical and spectrophotometric studies were performed with the $NaHSO_4$–$KHSO_4$ eutectic (50–50 weight ratio, m.p. 125°C).

Preparation of glasses and measurement of T_g values

It was found most convenient to prepare bisulphate glasses by careful melting of the solids in glass test-tubes above a cool bunsen flame, and then by cooling with compressed air or running water. (More conventional techniques using beakers heated on hot-plates cause water loss from the bisulphates and results are generally less satisfactory.) Glasses prepared in this way appear to be stable indefinitely at room temperature. Potassium bisulphate glasses have been prepared also in plate form by pouring onto a brass block, but attempts to prepare sodium–potassium bisulphate glasses in this way resulted in rapid devitrification, a phenomenon which appeared to be related to the uptake of water vapour from the air. Glass transition temperatures (T_g) were determined in the conventional way using a Dupont 950 Differential Thermal Analyser.

Electrolytic cells

(*a*) Electrolytic oxidations and reductions were performed in a 4-necked 500 ml reaction flask. Two electrode compartments were isolated from the bulk melt by glass frits (porosity 3) and this permitted anodic and/or cathodic solution products to be isolated. An auxiliary electrode and thermometer well were immersed in the bulk melt and this completed the cell. The flask was heated conveniently in an isomantle, and the temperature was controlled by a variac to ±2°C.

(*b*) The above cell was readily converted to a 3-electrode cell for voltametric experiments. One of the isolated compartments contained a silver/silver(I)(0·02m) reference electrode, and another the platinum microelectrode (surface area 0·05 cm^2). The platinum auxiliary electrode dipped directly into the bulk melt.

(*c*) For the determination of electrode potentials, the silver/silver(I) reference electrode (0·02m Ag^+) was used, and the other 'half-cells' were isolated in glass fritted compartments.

Electrical circuitry

Current for the electrolytic oxidations and reductions was drawn from a Solartron power supply (Model AS1218) and measured by a Sangamo Weston multirange milliammeter. A 3-electrode potentiostatic system was employed for the voltametric studies. The linear sweep in voltage between the micro- and reference electrodes was provided by a 'Hickling' potentiostat and electromechanical scanning unit, as supplied by Witton Electronics. The 'polarographic' current was recorded on a TOA, model EPR, pen recorder, which measured the voltage across a resistance in series with the auxiliary electrode. For the measurement of EMF values (for the electrochemical series) a Pye Portable Potentiometer was employed with the Hewlett Packard Voltmeter (Model DC419A) as null detector.

Spectrophotometric measurements

The electronic spectra of the various species dissolved in bisulphate glasses were recorded on a Unicam SP700C spectrophotometer. For obtaining accurate spectra, the glass was usually quenched inside a quartz optical cell, but for comparative purposes it was sufficient (and much less expensive) to obtain spectra with glasses quenched inside quartz or glass test tubes. (This latter method is described elsewhere [20].)

Results

Glass formation

Observations on glass forming properties in the $NaHSO_4$–$KHSO_4$ system revealed that good glasses can be obtained over the entire composition range; systems close to the eutectic composition are of most interest since in this region the melts show very little tendency to crystallize. Melts in the NH_4HSO_4–$NaHSO_4$ and NH_4HSO_4–$KHSO_4$ systems, however, were not good glass formers. Glass transition temperatures were determined as 310°K for $KHSO_4$, 297°K for $NaHSO_4$, and 298°K for $NaHSO_4$–$KHSO_4$ (eutectic); the closeness of these to ambient temperature is worth noting.

Redox phenomena in molten bisulphates

(*a*) *Spectrophotometric studies*

Table 1 contains spectroscopic data for a range of transition and post-transition metal ions dissolved in $NaHSO_4$–$KHSO_4$ glass. It is possible to detect a pattern in the redox chemistry and solvent properties of the melt. The available oxidation states are very similar to those which are thermodynamically stable in aqueous solution, but there does seem to be a trend for higher oxidation states to be more stable. For example, iron(II) is rapidly converted into iron(III), and vanadium(III) to vanadium(IV) and vanadium(V). Strong oxidizing agents such as dichromate permanganate and bismuthate(V)

Table 1. Spectrophotometric identification of ionic species in bisulphate glass

Metal	*Oxidation state*	*Compound added*	*Absorption spectrum*		*Stereo-chemistry*	*Assignment*	*Type of transition*	*Reference*
			$\nu_{max}(cm^{-1})$	ε_{max}				
Titanium	+4	TiO_2	39,000	12,000	tet	$(t_1\pi) \rightarrow e^*$	charge transfer	[18]
Vanadium	+4	$VOSO_4$	12,100	28	oct(VO^{2+})	$^2B_2 \rightarrow {}^2E(I)$	crystal field	[17]
			13,500 sh			$^2B_1$	crystal field	
			37,000 sh			$^2E(II)$	charge transfer	[18]
	+5	$NaVO_3$	28,400	2,300	tet	$t_1(\pi) \rightarrow e^*$	charge transfer	[18]
			47,600				charge transfer	
Chromium	+3	K_2CrO_4	14,400	27	oct	$^4A_{2g} \rightarrow {}^4T_{2g}$	crystal field	[17]
			15,000	28		$^2E_g(G)$		
			15,600 sh			$^2T_{1g}(G)$		
			21,400	31		$^4T_{1g}(F)$		
			32,400	20(a)		$^4T_{1g}(P)$		
	+6	K_2CrO_4(b)	49,700	16,300		$t_{1g}(\pi) \rightarrow t_{2g}^*$	charge transfer	[18]
Manganese	+2	$MnSO_4$	24,900	(c)	oct	$^6A_{1g} \rightarrow {}^4A_{1g}(G)$(c)	crystal field	[17]
	+3	$KMnO_4$	13,500	70	oct	$^5E_g \rightarrow {}^3T_{1g}(H)$	crystal field	[17]
			19,600	280		$^5T_{2g}$	crystal field	
			34,000	6,200		$t_{1g}(\pi) \rightarrow t_{2g}^*$	charge transfer	[18]
			43,600	8,100			charge transfer	
	+7	$KMnO_4$(d)						
Iron	+2	$FeSO_4$(e)						[17]
	+3	iron(III) alum	34,400	6,400	oct	$t_{1u}(\pi) \rightarrow t_{2g}^*$	charge transfer	[18]

Cobalt	+2	$CoSO_4$	6,600[f]		oct	$^4T_{1g} \rightarrow {}^4T_{2g}$	crystal field	[17]
			12,600	0·4		$^4A_{2g}$	crystal field	
			18,400	13		$^4T_{1g}(P)$	crystal field	
			20,500 sh					
Nickel	+2	$NiSO_4$	6,700	3·5	oct	$^3A_{2g} \rightarrow {}^3T_{2g}$	crystal field	[17]
			12,100	2·5		$^3T_{1g}$	crystal field	
			14,400	0·5		^1E_g	crystal field	
			23,200	8·3		$^3T_{1g}(P)$	crystal field	
Copper	+2	$CuSO_4$	11,600	27	oct	$^2E_g \rightarrow {}^2T_{2g}$	crystal field	[17]
			38,800	3,600		$t_{1u}(\pi) \rightarrow e_g^*$	charge transfer	[18]
Molybdenum	+5	$MoO(OH)_3$	13,400	(g)	oct (MoO^{3+})[g]	$^2B_2 \rightarrow {}^2E(I)$	crystal field	[21]
			22,100	(g)		$^2B_1$	crystal field	
Thallium	+1	Tl_2SO_4[h]	48,900	9,500	not known	$^1S_0 \rightarrow {}^3P_1$	Rydberg	[22]
	+3	Tl_2O_3	28,000 sh					
Lead	+2	$PbSO_4$	47,800	12,500	not known	$^1S_0 \rightarrow {}^3P_1$	Rydberg	[22]
	+4	$Pb(OAc)_4$[i]						
Bismuth	+3	Bi_2O_3	43,500	9,500	not known	$^1S_0 \rightarrow {}^3P_1$	Rydberg	[22]
	+5	$NaBiO_3$[j]						

---

[a] Approximate value owing to the presence of a slight concentration of chromium(VI) which absorbs strongly in this region. [b] Decomposes to chromium(III). [c] Owing to the feeble absorption of manganese(II), only the $^6A_{1g} \rightarrow {}^4A_{1g}(G)$ band was distinguished; its extinction coefficient could not be measured accurately. [d] Decomposes to manganese(III). [e] Decomposes to iron(III). [f] Approximate value owing to the rapidly increasing absorbance of the medium in this region. [g] Equilibrium between monomeric and dimeric forms exists. [h] Decomposes to thallium(I). [i] Decomposes to lead(II). [j] Decomposes to bismuth(III).

are decomposed by bisulphate melt, but it should be remembered that these species are thermodynamically unstable in aqueous solution also.

It is further apparent that the melt provides environments for dissolved ions similar to those in aqueous solutions. Thus the common transition metal cations, e.g. Mn^{3+}, Cr^{3+}, Fe^{3+}, Co^{2+}, Ni^{2+}, and Cu^{2+} all exist in sites of octahedral symmetry. Similarly, the frequencies of the s–p transitions observed for the ions Tl^{+}, Pb^{2+} and Bi^{3+} indicate that the ions possess very similar *ionicity* in bisulphate melts and in aqueous solution [22, 23]. (In contrast, these three ions are much more covalently bonded in chloride melts.)

Attempts were made to change the oxidation states of metal ions in the melt by electrolytic oxidation and reduction at 200°C and at platinum electrodes in order to generate species unobtainable by direct addition. These experiments, followed spectrophotometrically, were unsuccessful and it was not possible to produce any new species in this way. However, several 'reversible' redox couples were detected including Mn(III)/Mn(II), Mo(VI)/Mo(V), and V(V)/V(IV). The spectroscopic evidence for electrolytic oxidation of the vanadyl(IV) ion is illustrated in Fig. 1.

(*b*) *EMF measurements*

There are reports in the literature [6, 24] of the reversibility of the silver/silver(I) electrode in molten bisulphates, and this has been adopted as the reference electrode in this study. Consider the concentration cell:

$$\begin{array}{l} \text{Ag} \mid \text{Ag(I) melt} \mid \text{melt} \mid \text{Ag(I), melt} \mid \text{Ag} \\ \quad (0{\cdot}196\ \text{m}) \qquad\qquad\qquad m_x \end{array}$$

The concentration is expressed as a molality, i.e. g-ions of Ag(I) per 1,000 g of melt, Ag(I) being added as Ag_2SO_4. Fig. 2 shows that the EMF of this cell at 200°C varies with m_x in a manner consistent with the Nernst equation over a reasonable range of silver concentrations. The linear portion of the graph has a slope 0·094, which is identical within experimental error to the theoretical value. The useful range

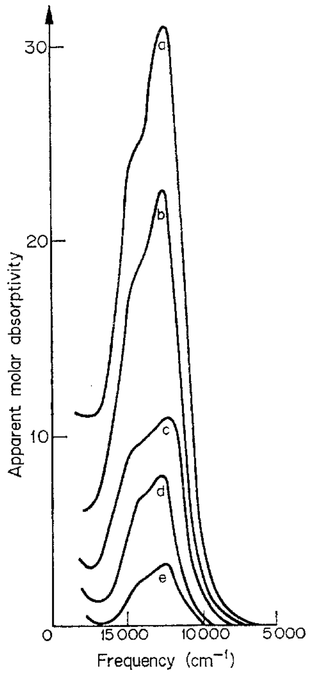

Fig. 1. Spectrophotometric evidence for electrolytic oxidation of vanadium(IV). Current was 5 mA and the spectra correspond to the following electrolysis times: (a) zero; (b) ¾ h; (c) 2½ h; (d) 4 h; (e) 12 h. (The presence of vanadyl(IV) ion is indicated by the absorption band with maximum at 12,100 cm^{-1}.)

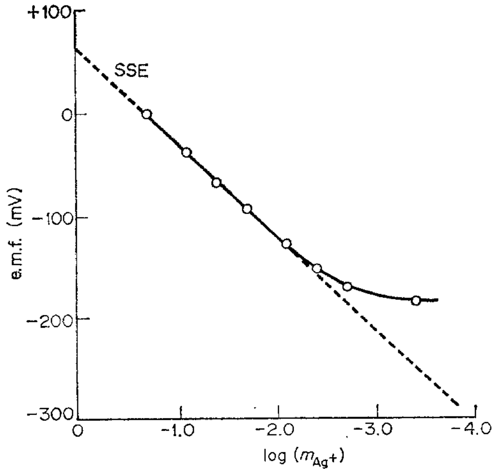

Fig. 2. EMF (in mV) of the cell Ag | Ag(I) (0·196 m), melt | melt | Ag(I)m_x, melt | Ag. The line with theoretical slope (0·094 V) is included (shown dotted), and this has enabled extrapolation to the standard silver electrode (SSE).

of Ag(I) concentrations is limited by the solubility of Ag(I) ions in the melt (0·2m) and by curvature in the Nernst plot at low concentrations—presumably caused by corrosion of the silver. It appears convenient to use a silver/silver(I) electrode with a concentration in the linear range of Fig. 2, but to refer all electrode potentials to the standard silver electrode (SSE), a hypothetical electrode, unimolal with respect to silver ion.

The Nernstian reversibilities of several metal/metal ion and redox electrodes were investigated in order to establish a simple electrochemical series in the molten bisulphate. The electrodes were chosen on the basis of the redox reactions which had been observed spectroscopically and also with reference to the reversibility of electrodes in aqueous systems. It is implicitly assumed that in this dilute solution range, the solutions are ideal, there being no evidence to the contrary.

Pt/V(V)/V(IV) electrode. The potential of this electrode was measured for V(V)/V(IV) concentration ratios varying from 0·33 : 1 to 15·9 : 1, (V(IV) concentrations in quenched glass measured spectroscopically), and over this range the Nernst equation was obeyed. Therefore

$$E = E^0_{\mathrm{V(V)/V(IV)}} + \frac{RT}{F}\ln\frac{[\mathrm{V(V)}]}{[\mathrm{V(IV)}]}$$

and

$$E^0_{\mathrm{V(V)/V(IV)}} = +0{\cdot}460 \text{ (with respect to SSE).}$$

Pt/Mo(VI)/Mo(V) electrode. The potential of this electrode was measured for Mo(VI)/Mo(V) concentration ratios varying from 1·75 : 1 to 55·0 : 1 (Mo(V) concentrations in quenched glass measured spectroscopically) and again over this range the Nernst equation was obeyed.

$E^0_{\mathrm{Mo(VI)/(Mo(V)}} = -0{\cdot}018$ V (with respect to SSE).

Pt/Mn(III)/Mn(II) electrode. This electrode is also found to obey the Nernst equation for a wide range of Mn(III)/Mn(II) concentration ratios (Mn(III) concentrations in quenched glass measured spectroscopically)

$E^0_{\mathrm{Mn^{3+}/Mn^{2+}}} = +0{\cdot}260$ V (with respect to SSE).

Pt/H$_2$/HSO$_4$– electrode. Arvia and Videla [6] have described the establishment of a reversible H_2 electrode on platinized platinum in molten bisulphates. This electrode was set up in the manner described, and it was found that $E_{\mathrm{H_2/HSO_4^-}} = +0{\cdot}195$ V with respect to SSE.

Cu/Cu^{2+} electrode. Gas evolution and copper dissolution is immediately detected on immersing copper wire in dilute solutions (*c.* 0·08m) of copper sulphate in bisulphate melt. The electrode potential is independent of the copper(II) concentration and comes to rest in the region $-0{\cdot}2$ V with respect to SSE.

Zn/Zn^{2+} electrode. Gas evolution and zinc dissolution are similarly observed on immersion of zinc electrodes in bisulphate melt. The electrode potential is independent of zinc concentration; the initial value is about $-1{\cdot}0$ V with reference to SSE but this rises to $-0{\cdot}4$ V in about 15 min.

Mercury/melt electrode. In connection with the possible use of the dropping mercury electrode (DME) for polarography (see below), the behaviour of a mercury pool electrode in contact with the melt was investigated. At the melt/liquid metal interface a moderate but continuous evolution of gas was observed, and very quickly the melt became cloudy with the formation of precipitate. Subsequent analysis of the bisulphate melt (dissolved up in water) indicated that the melt was heavily contaminated with mercury salts (formation of turbidity on addition of chloride ion). The mercury was obviously 'corroding' and the observed potential was $-0{\cdot}02$ V *v.* SSE.

Iron/melt electrode. Iron and stainless steel electrodes both appeared to show active–passive behaviour in the melt. The potential of both metals was observed to rise in a few minutes from about $-0{\cdot}6$ to $+0{\cdot}67$ V. The final rest potential of iron is interesting in that it is more positive than that of platinum; a similar phenomenon [25] is encountered for various metals which passivate in molten nitrates.

Aluminium electrodes were not examined here. Tajima *et al.* [1] reported that aluminium

Table 2. Electrode potentials of some metals and redox couples in $NaHSO_4$–$KHSO_4$ eutectic at 200°C

Electrode	$E°$ *(volts) v. SSE*	*Comments*
'Iron'	+0·67	passive electrode
$V(V)+e^- = V(IV)$	+0·460	reversible
$Mn(III)+e^- = Mn(II)$	+0·260	reversible
'Platinum'	+0·240	rest potential
$H^+ + e^- = \frac{1}{2}H_2$	+0·193	apparently reversible potential*
$Ag(I)+e^- = Ag(O)$	0	reversible
$Mo(VI)+e^- = Mo(V)$	−0·018	reversible
'Mercury'	(−0·02)	corrosion potential
$Cu(II)+2e^- = Cu(O)$	(−0·2)	corrosion potential
$Zn(II)+2e^- = Zn(O)$	(−1·0)	corrosion potential

* See ref. [6].

is rapidly coated with a porous though poorly conducting layer of α-alumina (corundum).

The information for these electrodes is summarized in Table 2. It is apparent that although there is a superficial resemblance between this series and the electrochemical series for aqueous systems (e.g. $E_{Zn^{2+}/Zn}$ is 1 V more negative than $E_{Cu^{2+}/Cu}$), there are important differences. Thus the hydrogen electrode is displaced in a positive direction with respect to other metal–metal ion electrodes—converting silver and copper into 'active' metals in this medium. This greatly reduces the number of reversible metal/metal ion electrodes which can be established because of interference from corrosion processes.

(*c*) *Voltametric studies*

Fig. 3 shows the limiting current-voltage behaviour of a 'blank' bisulphate melt at various temperatures, using the Ag/Ag(I)(0·02m) electrode as the reference and a platinum microelectrode as the working electrode. The range of electroactivity of the melt at 200°C is approximately from +0·25 V to +1·3 V (0·09 V to 1·14 V *v.* SSE), and it is apparent that only the vanadate(V)/vanadyl(IV) electrode has a potential which falls comfortably within this range.

The voltametric waves for anodic oxidation of vanadyl(IV) and cathodic reduction of vanadate(V) were obtained at a sweep rate of 50 mV/min., and show a half-wave potential of +0·49 V *v.* SSE for both anodic and cathodic waves, which is indicative of a reversible process. This can be written as

$$VO^{3+} + e^- \rightleftharpoons VO^{2+}, E_{\frac{1}{2}} = +0{\cdot}49 \text{ V}.$$

The half-wave potential (+0·49 V) is in good agreement with the standard potential (+0·46V); the difference can be accounted for in terms of the enhanced mobility of vanadyl ions relative to vanadate ions in the melt. Since both oxidized and reduced species are soluble in the melt, the current-voltage data for the voltametric wave should obey the Heyrovsky–Ilkovic equation if the process is reversible.

$$E = E_{\frac{1}{2}} + \frac{2{\cdot}303\, RT}{F} \log \frac{(i_d - i)}{i}$$
$$= E_{\frac{1}{2}} + 0{\cdot}094 \log \frac{(i_d - i)}{i} \text{ at } 200°\text{C}$$

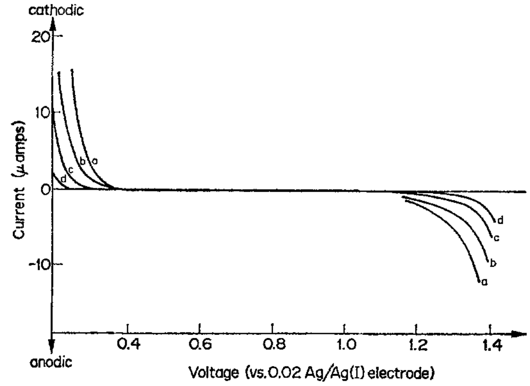

Fig. 3. Current-voltage behaviour at a Pt microelectrode (wire, 0·05 cm² surface area) in the $NaHSO_4$–$KHSO_4$ eutectic at various temperatures (180–240°C).

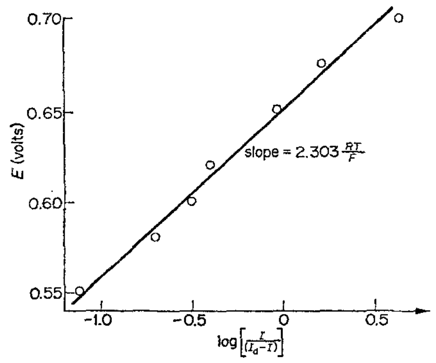

Fig. 4. Plot of E v. log $[I/(Id-I)]$ for the wave corresponding to the anodic oxidation of vanadyl (VO^{2+}) ion. The data fit the Heyrovsky-Ilkovic equation.

Fig. 4 shows that the data for the anodic oxidation of vanadyl(IV) do fit this equation quite satisfactorily.

Determination of Hammett acidity function

The determination of the acidity of concentrated sulphuric acid and other strong acids by examining equilibria for the protonation of weak bases is a well-established procedure (see for example [26]). This procedure has now been extended for the first time to molten salts to include the bisulphate system. Various weak bases were dissolved in the $NaHSO_4$-$KHSO_4$ melt and the resulting glasses were examined spectrophotometrically. By comparison with the spectra of the bases in 98% sulphuric acid and in ethanol, it was possible to decide whether or not the bases were protonated in the bisulphate glass. The results are shown in Table 3.

The Hammett acidity function, H_0, of a solvent is given by the equation

$$H_0 = pK_a + \log\frac{[B]}{[BH^+]}$$

where pK_a is known for a base/conjugate-acid pair. Weaker organic bases (pK < -2) appear to dissolve in the bisulphate melt only after sulphonation has occurred. However, *o*-nitroaniline dissolves straightforwardly and exists in the melt mainly as the conjugate acid, but a trace of the unprotonated form is also present. From the spectrum it was possible to estimate the value of the Hammett acidity function as lying in the range -1 to -2. To obtain a more precise figure for H_0 it would be necessary to 'titrate' hot concentrated H_2SO_4 with Na_2SO_4-K_2SO_4 mixture, and to observe a progressive change, but it was decided that this was outside the scope of the present study.

Miscellaneous effects

The redox properties of bisulphate melts can be altered to some extent by addition of certain reagents. Thus addition of sodium sulphite causes reduction of vanadium from oxidation state (V) to (IV). This reaction is probably related to the catalytic process for the oxidation of SO_2 to SO_3 in sulphuric acid manufacture.

Similarly, the addition of ammonium bisulphate inhibits aerial (or melt?) oxidation of vanadium(IV) to vanadium(V) and also of iron(II) to iron(III). These effects are not understood, but it does appear that the solvent properties of the NH_4HSO_4-$KHSO_4$ eutectic are rather different from those of the $NaHSO_4$-$KHSO_4$ eutectic. A study of free radical reactions in molten bisulphates by glow-discharge electrolysis has been performed in this laboratory [27] with particular reference to the NH_4HSO_4-$KHSO_4$ melt.

Discussion

The most striking features of molten bisulphate chemistry are the strong oxidizing power and acidity of the melt. These factors lead directly to a very simple pattern of redox chemistry, there being severe restriction in the range of oxidation states for the common metals. The melts are also corrosive towards metals (especially mercury) and this restricts the scope of electrochemical and electroanalytical measurements. For example, it is not possible to apply the technique of classical polarography using the dropping mercury electrode to this solvent. In contrast to this, the dropping mercury electrode has been used successfully in molten nitrates [28], media which are generally considered strongly oxidizing in character.

Table 3. Spectral features (frequencies in cm^{-1}, extinction coefficients in parentheses) of some organic bases in ethyl alcohol, 98% sulphuric acid and bisulphate glass

		Absorption maxima		*Bisulphate glass*	
Base	*pK*	*(unprotonated, in EtOH)*	*(protonated in 98% H_2SO_4)*	*absorption maxima*	*comments*
p-nitroaniline	+1·11	26,900 (15,200)	—	—	protonated
		—	38,000 (6,000)	38,200	
		43,800 (6,300)	—	—	
3,5-dinitroaniline	+0·23	26,200 (1,930)	—	—	protonated
		—	33,600 sh	32,000 sh	
		38,400 (11,200)	—	—	
		—	40,000 sh		
			44,000 (16,850)	39,600	
o-nitroaniline	−0·13	24,600 (5,300)	—	25,000(a)	protonated(b)
		36,000 (4,900)			
			37,200 (7,300)	37,700	
		43,000 (16,600)	—	—	
		—	46,800 (5,800)	46,400 sh	
2,6-dichloro-4-nitroaniline	−2·55	28,000 (13,700)	—	—	(c)
		—	32,400 sh 38,400 (13,100)	36,000	
		44,500 46,000 sh 48,200 (20,500)	46,400 (37,000)	46,000	
2-nitrodiphenylamine	−4·12	24,000 (6,600)	—	25,400	(c)
		35,000 sh 38,700 (14,300)	37,300 (14,500)	35,000 sh 37,200	
2,4-dinitroaniline	−4·38	26,500 sh 30,000 (14,800)	—	25,600 sh 28,400	(c)
				33,500	
			34,300 sh	37,200	
		39,200 (9,800)	42,800 (1,500)	41,400	
		45,000 (10,500)			
Anthraquinone	−8·15			insoluble	bisulphate melt insufficiently acidic to dissolve base

(a) Very weak band. (b) A small proportion of base is protonated. (c) These bases are only sparingly soluble until sulphonation occurs.

The solution chemistry of molten bisulphates is readily studied, however, by taking advantage of the ease with which the melts can be quenched to glasses and investigated spectrophotometrically. By reference to Table 1 it is possible to get detailed information about a wide range of solute species in the bisulphate melt. In general (see above) the species resemble those in aqueous solution rather than in anhydrous molten-salt systems. The difference can be summarized by the statement that whereas in many molten salts the spectroscopic data can be interpreted as indicating the formation of specific 'complexes', e.g. $[CoCl_4]^{2-}$[29], $[Co(NO_3)_4]^{2-}$ [30, 31] and $[Co(OAC)_4]^{2-}$ [32], in the bisulphate melt and in aqueous solutions the typical cations, e.g. Co^{2+} and Pb^{2+}, are more *ionic* in character, and are 'solvated' rather than complexed.

The restricted range of oxidation states available to each element can be explained in terms of the high acidity and low water activity in the melt. These properties will for example enhance the instability of oxyanion species, since reduction involves the conversion of oxide ligands into water. This is seen in the reduction of dichromate, which may be written as:

$$Cr_2O_7^{2-} + 8H^+ = 2Cr^{3+} + 4H_2O + \tfrac{3}{2}O_2$$

In similar manner, the sulphate ion behaves as a mild oxidizing agent in the melt. It is for this reason that some low oxidation states stable in aqueous solution are unstable in the melt, and that the gaseous reaction product is so often sulphur dioxide. Thus, oxidation of iron(II) to iron(III) occurs *via* sulphate reduction and can be written as:

$$SO_4^{2-} + 2Fe^{2+} + 4H^+ = SO_2 + 2Fe^{3+} + 2H_2O$$

The corrosion of metals in molten bisulphates is complicated by the possibility of both H_2 and SO_2 evolution, and this aspect of electrochemistry in molten bisulphates deserves further study.

In this study we have attempted to lay the groundwork for the use of molten bisulphate as a solvent and as a glass/melt system. The pattern of redox chemistry is apparently very simple, but recent experiments performed in this laboratory indicate a wider range of chemical reactions for the platinum group metals. These systems are to be investigated and will be discussed in a future paper.

Acknowledgments

One of us (S.M.F.) wishes to thank the University of Aberdeen for the award of a Maintenance Grant. We are also indebted to Mr. G. G. Lewis for measuring glass transition temperatures and Mr. A. McLeman for some practical assistance.

References

[1] S. E. Rogers and A. R. Ubbelohde, *Trans. Farad. Soc.* **46**, 1051 (1950).
[2] S. Tajima, M. Soda, T. Mari, and N. Baba, *Electrochim. Acta* **1**, 205 (1959).
[3] A. M. Shams el Din, *ibid.* **7**, 613 (1962).
[4] A. J. Arvia and H. A. Videla, *ibid.* **10**, 21 (1965).
[5] A. J. Arvia and H. A. Videla, *ibid.* **10**, 33 (1965).
[6] A. J. Arvia and H. A. Videla, *ibid.* **11**, 537 (1966).
[7] A. J. Arvia, A. J. Calandra, and H. A. Videla, *ibid.* **13**, 167 (1968).
[8] A. J. Arvia, F. De Vega, and H. A. Videla, *ibid.* **13**, 581 (1968).
[9] A. J. Arvia, A. J. Calandra, and H. A. Videla, *ibid.* **14**, 25 (1969).
[10] L. Cambi and G. Bozza, *Ann. Chim. Appl.* **13**, 221 (1923).
[11] D. Tomkova, P. Jiru, and J. Rosicky, *Coll. Czeck. Commun.* **25**, 957 (1960).
[12] G. E. Walrafen, D. E. Irish, and J. F. Young, *J. Chem. Phys.* **37**, 662 (1962).
[13] T. Forland and W. A. Weyl, *J. Am. Ceram. Soc.* **33**, 186 (1950).
[14] J. A. Duffy, F. P. Glasser, and M. D. Ingram, *J. Chem. Soc.* **A**, 551 (1968).
[15] C. A. Angell and C. T. Moynihan, in 'Molten Salts, Characterization and Analysis', p. 315. Ed. Gleb Mamantov, Marcel Dekker (1969).
[16] R. Bose, R. Weiler, and P. B. Macedo, *Phys. Chem. Glasses*, **11**, 117 (1970).
[17] J. A. Duffy and W. J. D. Macdonald, *J. Chem. Soc.*, **A**, 977 (1970).
[18] J. A. Duffy and W. J. D. Macdonald, *Phys. Chem. Glasses*, **11**, 1 (1970).
[19] J. A. Duffy and W. J. D. Macdonald, *J. Chem. Soc.*, **A**, 2066 (1970).
[20] J. A. Duffy, and M. D. Ingram, *Chem. Instrum.* (to be submitted).
[21] J. A. Duffy, *Phys. Chem. Glasses* **9**, 190 (1968).
[22] J. A. Duffy, S. M. Forbes, and M. D. Ingram, *J. Chem. Soc.* **A**, 452 (1970).
[23] J. A. Duffy and M. D. Ingram, *J. Chem. Phys.* (in press).
[24] R. P. Seward and J. P. Miller, *J. Phys. Chem.* **69**, 3156 (1965).
[25] A. Conte and S. Casadio, *Ric. Sci.* **36**, 433 (1966).
[26] P. A. H. Wyatt, 'Annual Reports', *Chem. Soc.* (1969), p. 93.
[27] L. W. Hamilton and M. D. Ingram (unpublished work).
[28] G. Tridot, G. Nowogroki, J. Nicole, M. Wozniak, and J. Canonne, *C.R. Acad. Sci. Paris, Ser. C* **270**, 204 (1970).
[29] D. M. Gruen and R. L. McBeth, *Pure Appl. Chem.* **6**, 23 (1963).
[30] J. A. Duffy and M. D. Ingram, *J. Am. Ceram. Soc.* **51**, 544 (1968).
[31] K. W. Fung and K. E. Johnson, *Can. J. Chem.* **47**, 4999 (1969).
[32] J. A. Duffy and M. D. Ingram, *J. Chem. Soc.* **A**, 2398 (1969).